Digest Journal of Nanomaterials and Biostructures Vol. 9, No. 3, July - September 2014, p. 1223 - 1231

SPECTRAL CHARACTERISATION OF THE OLIGODYNAMIC LIMIT EVOLUTION FROM Ag^+ TO Ag NANOSIDED PARTICLES IN BSA SOLUTION

A. IOANID[a], S. ANTOHE[a,b,*]
[a] *University of Bucharest, Faculty of Physics, 405 Atomistilor Street, PO Box MG-11, 077125, Magurele-Ilfov, Romania*
[b] *Academy of Romanian Scientists, 54 Splaiul Independenței, Bucharest*

Clinical experience shows that the effective concentrations of a total oligodynamic Ag^+ in vivo must assure the target tissue load of from 1 ppm to 10 ppm, namely required a picoscalar Ag^+ content, that is from 10^{-6}M to 10^{-5}M in solution. We present an analysis of the interaction mechanisms between Ag^+ and BSA molecule in solution, at constant BSA:Ag stoichiometry, by time-dependent UV-Vis absorbance recording. Time evolution of the effect of bonded Ag^+ at BSA sites has two steeps: first one of binding to protein molecule and second one of competitive Ag-Ag specific interaction that favorises metallic clustered formations with size stabilized by the double layer potential generated by anions protein adsorption on the Ag seeds surface. Finally, the solution contains some Ag nanoparticles as core-shell type, Ag-BSA capped layer. Ag clusters formation is favorized by the Ag excess delivered by the UV photodegradation of the Ag complexes. The bioactivity is substituted by toxicity for a critical size of initial Ag clusters, that essentially depends on the Ag^+ concentration in solution. The large size seeds is not assimilated with biological medium.

(Received June 2, 2014; Accepted September 27, 2014)

Keywords: Oligodynamic content, S-S bond, Ag-Ag interaction, Ag small clusters, Plasmon mode frequency

1.Introduction

Since ancient times, antimicrobial effects of silver and its compounds were known and used, but hardly on the ninetheenth century end it has been established that only oligodynamic silver is biologically active, namely oligodynamic ion (Ag^+) content has great efficiency in viral and bacterial conditions. At nanotechnology era, the modern methods perform the oligodynamic nano-Ag sources used as a powerful, both the antimicrobial agent and preventative against most human infections, due to surface area and surface energy thermodynamics [1,2]. Clinical experience shows that the effective concentrations of a total oligodynamic Ag^+ in vivo must assure the target tissue oad of from 1 ppm to 10 ppm, namely required a picoscalar Ag^+ content, that is from 10^{-6}M to 10^{-5}M in solution [3]. The most biologically useful picoscalar Ag^+ speciation is the colloidal silver hydrosol that improves the safety and efficacy on the Therapeutic Index of Ag^+ activity [4]. Both the charge and very low size assure in vivo great mobility of the Ag^+ inclusive by the cellular membrane channels, but the antimicrobial efficiency is due to their specific interactions with the target molecule (e.g., bacteria) that bring in their complexation and influence both their conformational and functional stability [5]. On the other hand, the clinical practice shows that the efficiency is time dependent, so that a small dose must be administered for long time, while a fast efficiency is obtained using any high doses that increase the risk of large sediments with toxic effects. Most advanced medical applications use Ag nanoparticles with specific characteristics that can be synthesized and stabilized in vivo by peptides, proteins, DNA, and chemical or biological polymers [6].

*Corresponding: santohe@solid.fizica.unibuc.ro

In vivo interactions between the Ag^+ and the biomolecules, as seric albumines, enzymes, bring in their decoration by binding and consequently, in their reactivity increasing by notable configurational and functional changes [7]. In both the human and animal biological medium, the seric albumines are the most abundant and main proteins that transport both the oxygen and drug. The strength of the tertiary structure that assures normal function of proteins, is provided by a specific disulphides bonds (S-S) number. Referring to BSA, then the physiological environmental conditions and the binding of ligands change the molecule shape breaking some disulphide bonds, this regains easily its native shape reestablishing these bridges [8].

It is known that the heavy metal ions, as Hg^{2+}, Pb^{2+}, Ag^{+1}, Tl^{+1}, Cd^{2+}, with high affinity for sulfur form metal-sulfur bond that is stronger than bonds with other functional groups as amines, carboxylic acids, alchohols and phosphors of protein molecule [9]. The interaction between the Ag^+ and proteins is mainly due to their affinity for sulfur, so that the Ag^+ neighbourhood induces the S-S bond cleavage and consequently any the molecule conformational changes associated with his physical and functional properties changes [10]. According to the structural chemistry of the Ag^+, this has a pronounced nitrophylic character, so that forms numerous nitrogen atoms coordination complexes [11].

The Ag^+ has high affinity for other donor functional groups of the proteins, as that with nitrogen $–NH_2$, N-C, or –COOH, -CO groups, forming via covalent bonds a large range of Ag complexes. These are resistent towards visible leight, but after the exposure to UV radiation, are photodegradaded delivering metallic Ag that forms a colloid suspension of nanosized particles [12].

Although with low rate, the exposure to UV radiation enhances breaking of the Ag complexes, followed by photoreduction of Ag^+ to Ag and seeds deposition [13,14]. These seeds are clusters that may evoluate on two ways. First way, whitout other oxidized agents adding, the seeds become nanodevices as core- shell, here Ag-BSA that may be used, for exemple, as biosensors for recognizance of a target molecule, by the significant RET couplage Förster distance increase [15]. The nanodevices efficiency for this function depends to oxidized agent, so that, e.g., for the HIV or Ecoli as target the efficiency of Ag-BSA is lower that than of Ag-PVP(poly(vinylpyrrolidone)) nanodevices [16]. Moreover, the seeds aggregation is favorized by the Ag specific property named argentophilicity [17] consisting to strong Ag-Ag interaction with U_{Ag-Ag} = 20 kJ/mol energy bond.

Second way, the initial Ag seeds, with sizes and shape depending on the Ag^+ concentration in solution, play rôle of germs for the particle growth by photoreduction process.

It is known that the Ag nanosized exhibits stronger and sharper plasmon resonance peaks than other metals(e.g., gold)[18]. The plasmon mode frequency depends on environment and for a given solvent, depends on both the nanoparticles shape and size. Then the size increases, the plasmon frequency shifts to longer wavelength [19]. By irradiation with the wavelenght associated to the seed plasmonic electronic mode frequency, the photovoltage created on the seed attracts the Ag^+ ions to cathode and their reduction greatly enhances the rate deposition to Ag (prisms or hexagonal) nanocrystals [13,14]. Growth efficiency depends on solvent environmental because the Ag^+ traped by nanoparticle photovoltage must penetrate the double electrical layer of Ag coated seeds. Spherical Ag nanoparticles with average size of 3 to 8 nm seeds by Ag^+ reduction have been detected for 10^{-5} to 10^{-6}M $AgNO_3$ in solution [20].

We present an analysis of the interaction mechanisms between Ag^+ and BSA molecule in solution, at constant BSA:Ag stoichiometry, by time-dependent UV-Vis absorbance recording. Time evolution of the effect of bonded Ag^+ at BSA sites has two steeps: first one of binding to protein molecule and second one of competitive Ag-Ag specific interaction that favorises metallic clustered formations with size stabilized by the double layer potential generated by anions protein adsorption on the Ag seeds surface. Finally, the solution contains some Ag nanoparticles as core-shell type, Ag-BSA capped layer.

As above comments, the Ag clusters formation is favorized by the Ag excess delivered by the UV photodegradation of the Ag complexes [13,14]. The bioactivity is substituted by toxicity for a critical size of initial Ag clusters, that essentially depends on the Ag^+ concentration in solution. The large size seeds is not assimilated with biological medium.

We have choose the BSA protein molecule because is like as homologus human serum albumin (HSA), is most abundat protein in blood plasma helps in transport of drugs and ligands, but has low cost, availability and high affinity for metal ions.

2.BSA-Ag binding considerations

2.1. Ag^+ - S-S interaction

Disulfide S-S is a covalent bond formed by oxidation breaking of functional sulfhydril (or thiol) groups $(-SH)$ in keeping with equation $(R-SH)+(R'-SH)\rightarrow R-S=S-R'$, where R and R' are cysteine residues. According to the cysteines position belong to distinct protein molecules or the same protein chain, the S-S bonds are interchain or intrachain. Both the inter- and intrachain S-S bonds type have been categorised as structural, catalytic or allosteric, according to their folding and stabilization of proteins rôle, regulation of their enzymatic activity or function flexibility, respectively [10]. BSA is a single polypeptide whose molecule contains 582 amino-acids residues among that 35 are cysteine residues. In native physiological conditions, the secondary structure of molecule is stabilized by 17 intrachain cysteine-cysteine S-S bonds resulting in 9 loops delimited by the bridges S-S, while one cysteine is outside residue exposing a strong reactiv free thiol $(-SH)$ group [20,21]. By chemical treatment of BSA, e.g., adding of sodium borohidride ($NaBH_4$) as reduced agent, most its S-S bonds are converted to $(-SH)$ groups, so that new denaturated dBSA molecule has more reactivity [22].

Due to the Ag^+ ion high affinity to S, the bonding Ag-S prevails to S-S bonding. For exemple, from the SERS spectrum of the self-assambled monolayer of diphenyldisulfide (DDS) on polycristalline Ag film, the frequencies associated to lateral S-S bonds $(\sim 340 cm^{-1})$ disappear, while appear the frequencies associated to the vertical S-Ag bond $(\sim 1571 cm^{-1})$ [23]). The strong coordination Ag---S-R on the one hand and the strong Ag-S affinity on the other hand, produce a long-chain of inorganic compounds $(-S-Ag-S-)$, flanked by self-assambled biomolecules layers [24].

Molecule shape modified by the reduction of the S-S bridges number and breaking of some 9 loops, is one linear with large exposure area to solvent and lower electrophoretic mobility [25].The molecular conformational change improves orientational dielectric relaxation processes of both the protein molecule and solvent, so that the kinetics shows long time (up to $\sim 300 min$) hysteresis effects. This feature must be considered for based drug Ag metabolism and transportation because binding by metal ion can make the drug more active and less toxic [26]. In Ag case, one source of toxicity is the Ag seeds aggregation by strong Ag-Ag interaction. Besides the antimicrobial effect of the Ag^+ to BSA sites, this is used as selective Ag^+ probe. So that, for exemple, the fluorecence of the water-soluble CdSe capped by BSA is quenched by Ag^+ neighbouhood [27]. The strongest protein interactions with Ag^+ that involve the thiol-bearing cysteine residues of BSA, stabilize Ag nanoparticles of 2-3 nm in diameter [16].

2.2. Ag-Ag intraction

The strong interaction Ag^+ - SH results in a linear di-coordinate complexes $(-S-Ag-S-)$, that can link through Ag-Ag interaction, Fig.1.a., and aggregate to form Ag colloid suspensions of nano-size particles, or Ag clusters, that for high level Ag^+ concentration, seed in solution [28].

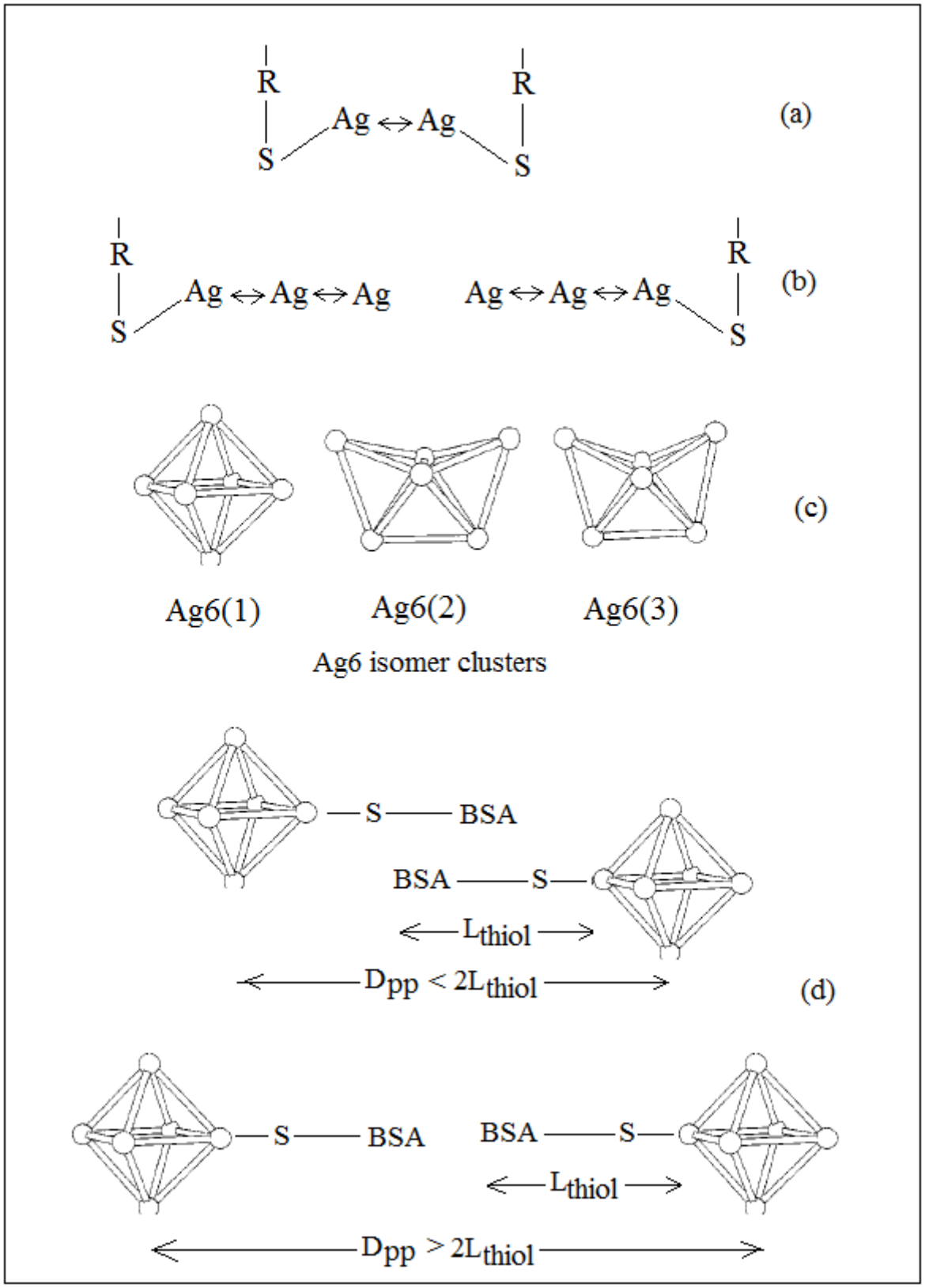

Fig.1.Evolution outline of the Ag^{+} concentration in BSA buffer solution after UV exposure: (a) $Ag-S(BSA)$ *complexes linkage by Ag-Ag interaction; (b) Ag clusters growth by excess photodegradation delivered Ag-Ag interaction; (c) Ag small cluster isomers[30] ; d) interaction between Ag nanoparticles capped with BSA*

Moreover, an Ag quantity is delivered in solution by photodegradation of others weakly bound Ag complexes. The Ag aggregates formation is favorized by the specific metallophilic Ag-Ag interaction resulting in Ag-Ag dimer with the energy bond $U_{Ag-Ag} = 20 kJ/mol$ and the interatomic distance $d = 2.88 Å$ [12], while the bulk Ag lattice parameter is $a = 4.07 Å$. Although the energy bond $U_{Ag-S} = 217 kJ/mol$ [29] is of ten time more than U_{Ag-Ag}, the aggregation to nanoparticles as Ag cluters by Ag-Ag interaction is competitive due to abundance of Ag delivered by Ag complexes photodegradation(Fig.1.b.). Smaller size of a Ag lowest-energy configuration cluster is $n = 6$ and has three isomers, Fig1.c [30].

Clusters average size is stabilized by the electrical double layer generated by the neighbourhood of BSA molecules in solution, so that a new phase of Ag nanoparticles $BSA(-SH)$-capped Ag nanoparticles appears, Fig.1. d. For the same $(-SH)$ source, the $BSA(-SH)$-capped Ag nanoparticles have contact-free distribution or become nanoparticles aggregates, depending on their concentration. It is resonable to consider that for low (oligodynamic limit) initial Ag^+concentration, after to UV exposure small $BSA(-SH)$-capped Ag nanoparticles are obtained, so that the interparticle distance $D_{PP} >> 2L_{thiol}$ and the interparticles interaction is canceled.

3. Experimental results

We present an analysis of the time-depending UV spectra of the $5 \times 10^{-5} M\,[BSA : Ag] : [1:1]$ solution recorded in the wavelength range of $(200 \div 600) nm$, at certain time intervals in time range of $(0 \div 300)$ minutes. Solution were prepared adding BSA with electrophoretic purity purchased from Sigma Laboratories and silver nitrate p.a. ($AgNO_3$) from Reactivul Laboratories as precoursor of Ag^+ in the phosphate buffer solution with the $pH \in (7 \div 7.4)$. Spectra were recorded as difference absorbance spectra beetwen $5 \times 10^{-5} M\,[BSA : Ag] : [1:1]$ sample cell and $5 \times 10^{-5} M\,[BSA]$ reference cell using a Perkin Elmer Lambda 35 Spectrofotometer, considering as origine time $(t = 0 \min)$ the starting moment of the first spectrum, in ambiental conditions. At first, in Fig.2 we present the UV absorbance spectra recorded in the same conditions, as integral spectrum for pure BSA/air (1) and $[BSA : Ag]/air$ (2), and as difference spectrum for $[BSA : Ag]/BSA$ (3) buffer solutions.

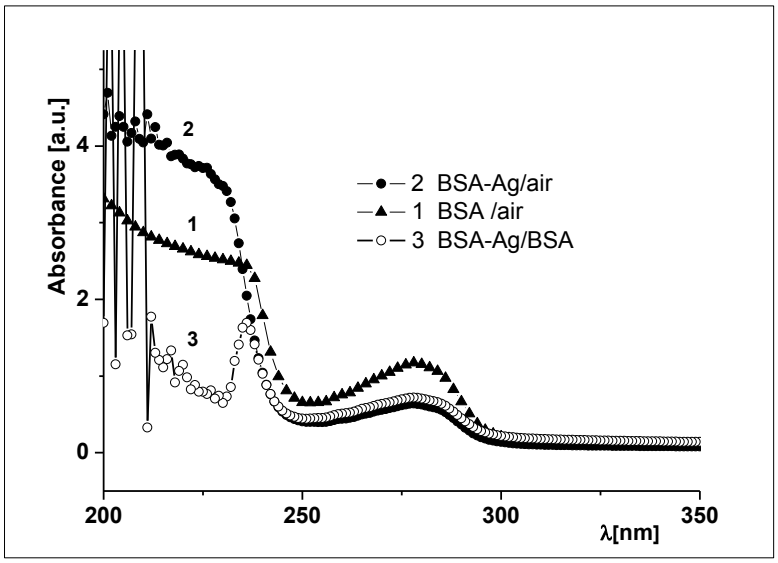

Fig. 2. The UV-absorbance spectra: (1) BSA/air *solution ; (2)* $[BSA : Ag]/air$ *solution; (3)* $[BSA : Ag]/BSA$ *solution*

In Fig.3 we present the difference absorbance spectra recorded for several time moments of $(0 \div 300)$ minutes range, considering every time value as spectrum starting moment.

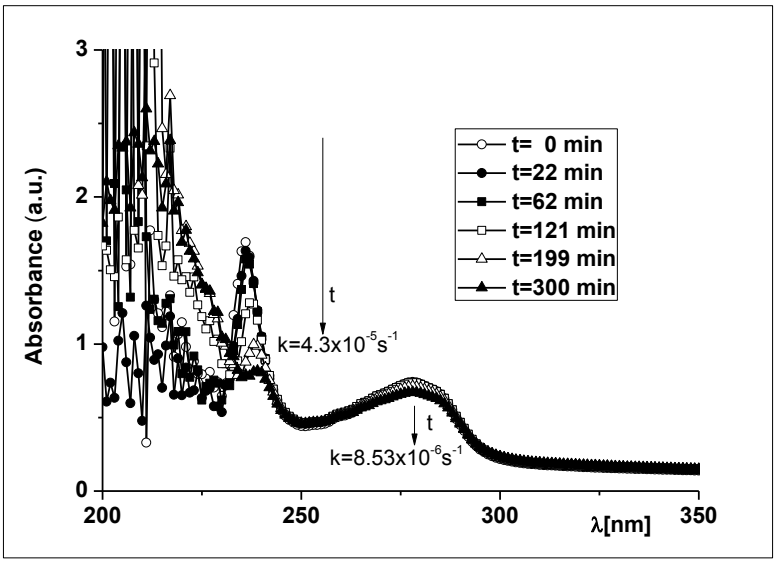

Fig. 3. The time-depending UV difference absorbance spectrum of the 5×10^{-5} M $[BSA : Ag]:[1:1]$ *solution. The narrows show the increasing time*

4. Discussions

All the three spectra (Fig.2), show both the specific at ~ 280nm peak and ~ 240nm intrinsec absorbance edge of BSA due to their amide groups electronic transitions, but with different features for $[BSA : Ag]$ solution. Thus, the ~ 280nm peak absorbance of the $[BSA : Ag]$ solution is lowered, while below 240nm the absorbance of the $[BSA : Ag]$ solution is greater than that for BSA solution. Moreover, the $[BSA : Ag]/BSA$ difference spectrum has a pronounced peak at ~ 240nm. Accommoding the Beer-Lambert law to the absorbance (A) time dependence (Fig.3), the rate constant of each peak evolution has been obtained as the slope of the linear fitting time dependence of logA. So that, while the 280nm peak intensity decreases with rate constant $k_{280} = 8.53 \times 10^{-6} s^{-1}$, the 240nm peak decreases fastly with the rate constant $k_{240} = 4.3 \times 10^{-5} s^{-1}$.

It is known that the 280nm peak represents the characteristic absorbance of the hydrophobic chromophore residues tryptophan(Try) and tyrosine(Tyr) occupying interior sites of the native BSA molecule. Intensity decrease of this peak both for the single absorbance $[BSA : Ag]$ solution spectrum and for difference absorbance $[BSA : Ag]/BSA$ successive spectra, evidences any changes of the chromophore residues exposure to solvent induced by conformational changes of BSA molecule due to the binding of the Ag^+ with side-chain protein groups [31]. The 240nm absorbance peak proofs the existence of any Ag complexes photoexcitated with this wavelength, and the intensity decrease of each successive spectrum, shows that the absorbent centers number decreases also. Influence of the BSA molecule deformation is slowly because the binding of the Ag^+ to their $(-SH)$ free group enhaces long-time hysteresis processes specific to biomolecules dynamics [7]. Contrary, the photodegradation of the complexes formed by binding Ag^+ to others side-chain groups followed by Ag^+ to Ag conversion, is fastly and favorises Ag seeds. These considerations support the value of $5 \div 6$ for the k_{240}/k_{280} ratio. Moreover, we can estimate the thermodynamics parameters of both the conformational change of BSA molecule and Ag seeds deposition, using their rate constants, k_{280}

and k_{240}, respectively. Thus, in the first-order kinetics approximation, the process equilibrium constants is $K_{280(240)} = \frac{hk_{280(240)}}{k_B T}$ and the corresponding free energy Gibbs variation is $\Delta G_{280(240)} = -RT \ln K_{280(240)} = -RT \ln \frac{hk_{280(240)}}{k_B T}$, where k_B is the Boltzmann constant, h is Planck's constant and R is the universal gas constant. On the other hand, $\Delta G_{280(240)} = \Delta H_{280(240)} - T\Delta S_{280(240)}$ where $\Delta H_{280(240)}$ and $\Delta S_{280(240)}$ are the enthalpy and entropy variations for each process, at the same temperature T. The positive obtained values, $\Delta G_{280} = 102.24 kJ/mol$ and $\Delta G_{240} = 98.52 kJ/mol$ proof that both the conformational change of BSA molecule and Ag seeds aggregation are activated by the exposure to UV. Because for isothermal conditions the enthalpy variation is unchanged, results that both the processes occur mainly with entropy variation, $\Delta S_{280} < 0$ and $\Delta S_{240} < 0$, but $\Delta S_{280} < \Delta S_{240}$.

The loss configurational entropy after BSA molecule complexation by binding Ag^+ to other than $(-SH)$ group is greatest than that for Ag^+ -SH bond, and consequently the molecule returns fast to equilibrium conformation, while more stable Ag^+ - S-R bond plays rôle of germ for Ag seeds aggregation.

Ag colloidal seeds are small clusters those structural, chemical, termodynamic, electronic and optical properties depend essentialy on both their size (atoms number) and shape [32]. In point of optical, the presence of the small particles in solution may be proofed by the surface plasmon electronic mode specific to their size and shape. Moreover, the spectral shift of this surface mode from the bulk value $(\sim 340nm)$ is associated to size and shape changes, e.g., an the average diameter increase produces a red-shift [14,32]. Time-dependent absorbance spectrum in the surface plasmon mode wavelength range is shown in Fig.4 .

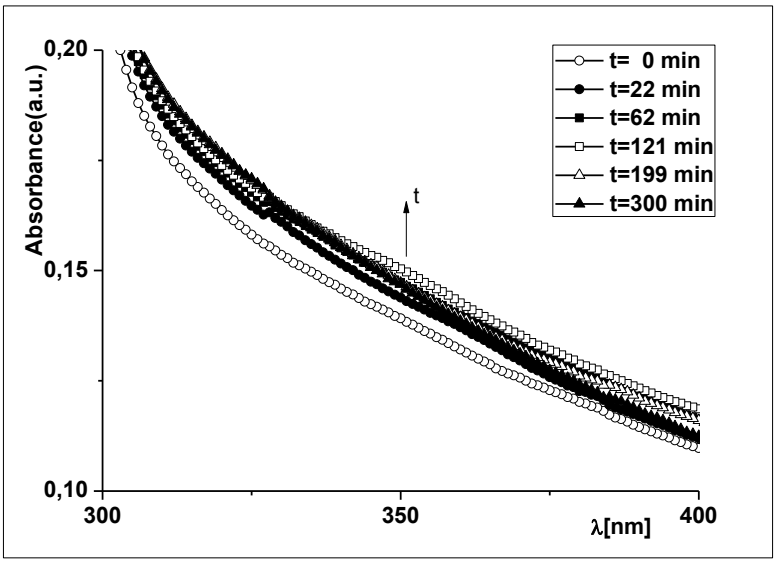

Fig. 4. The time-depending UV difference absorbance spectrum of the $5 \times 10^{-5} M$ [BSA : Ag] : [1:1] *solution in spectral range of Ag nanoparticles surface plasmon mode*

Successive absorbance increases and a should profiled at $(\sim 340nm)$ after one hour (62 minutes) shifts to $(\sim 350nm)$ after two hours (121 minutes). This small but discernable absorbance increase indicates the formation of smallest Ag clusters, while the long after a (300 minutes) attenuation is due to his coverage of BSA shell via the above described Ag^+ -SH interaction.

Both the 280nm and 240nm absorbance properties characterise the [BSA : Ag] solution system for low (oligodynamic) Ag^+ concentration values. For high precoursor of Ag^+ concentration in solution ($\sim 10^{-4}$ M of $AgNO_3$) [13] and using either reagents, oxidized or capped agents [18], the small colloidal seeds are converted to large nanocrystalline clusters, with plasmon excitations tunnable in both perpendicular and plane mode [13,14].

5. Conclusions

Ag biological activity for oligodynamic Ag^+ concentration consists to both that of the charged Ag^+ and neutral (or partial neutral) nanoparticles as small clusters capped with BSA. The Ag^+ activity is due to their high affinity for sulfur, binding either free (–SH) side-chain group or S-S bond of a target protein molecule, while the Ag nanoparticles are stabilized by a protein shell. While the UV exposure reduces the Ag^+ activity by Ag complexes photodegration and seeds deposition, the embeded Ag nanoparticles have specific interactions with target molecule via their expounded specific surface plasmon mode. Use the antimicrobial effect of oligodynamic Ag^+ must take in attention the slow conversion (~one hour) of the Ag^+ content to Ag nanoparticles.

References

[1] Rajani Shrestha, Dev Raj Joshi, Jyotsna Gopali, Sujan Piya, Nepal Journal of Science and Technology, **10**, 189 (2009).

[2] Kim, Keuk-Jun,Woo Sang Sung, Seok-Ki Moon, Jong-Soo Choi, Jong Guk Kim, Dong Gun Lee, J. Microbiol. Biotechnol., **18**(8), 1482 (2008).

[3] Eric J. Rentz, Journal of Nutritional & Environmental Medicine, **13**(2), 109 (2003).

[4] Goetz A, Tracy RL, Harris FS, Oligodynamic effect of silver, In Addicks L (ed) Silver in Industry, New York Reinhold, p.402-3,1940

[5] Ling-Zhi Wu, Bao-Liang Ma, Da-Wei Zou, Zuo-Xiu Tie, Jun Wang,Wei Wang, Journal of Molecular structures, **877**, 44 (2008).

[6] B.Sengupta, K. Springer, J.G. Buckman, S.P. Story, O.H.Abe, Z.W. Hasan, Z.D. Prodowsky, S.E. Rudisill, N.N. Degtyareva, J.T. Petty, J.Phys. Chem. C, **113**, 19518 (2009).

[7] Shen Xingcan, Yuan Qi, Liang Hong, Yan Haigang & He Xiwen, Science in China (Series B) **46**(4), 386 (2003).

[8] Maria Zavodszky, Chao-Wei Chen, Jeno-Kuen Huang, Michal Zolkiewski, Lisa Wen, Ramaswamy Krishnamoorthi, Protein Science,.10, p 140-160, 2001

[9] Goldys and Krystyna Drozdowicz-Tomsia, http://www.intechopen.com/books/nanowires-fundamental-research/gold-and-silver-nanowires-for-fluorescence-enhancement, 2001

[10] Mikael J. Lindberg, Johana Normark, Arne Holmgren, Mikael Oliveberg, Biochemistry, **101**(45), 15893 (2004).

[11] G.L. Miesler, D.A. Tarr, Inorganic Chemistry, 3rd ed, Prentice Hall, Englewood Cliffs, NJ, USA, 2004

[12] Nikolay Gerasimchuk, Polymers, **3**, 1475 (2011)

[13] Xiaomu Wu, Peter L. Redmond, Haitao Liu, Yihui Chen, Michael Steigerwald, Louis Brus, J.Am.Chem.Soc., **130**, 9500 (2008).

[14] Mingzhu Liu, Mei Leng, Chao Yu, Xin Wang, Cheng Wang, Nano.Res. **3**(12), 843 (2010)

[15] Joanna Malicka, Ignacy Gryczynski, Jozef Kusba, Yibing Shen, Joseph R. Lakowicz, Biochemical and Biophysical Research Communications, **294**, 886 (2002).

[16] Jose luis Elechiguerra, Justin I.Burt, Jose R. Morones, Alejandra Camacho-Bragado, Xiaoxia Gao, Humberto H Lara, Miguel Jose Yacaman, Interaction of silver nanoparticles with HIV-I, Journal of Nanobiotechnology **3(**6), 2005, http://www.jnanobiotechnology.com/content/3/1/6

[17] M.Dennehy, O.V.Quinzani, R.A.Burow, Acta.Cryst., **63**, 395 (2007)

[18] Anitha Sironmani and Kiruba Daniel, Silver Nanoparticles-Universal Multifunctional

Nanoparticles for Bio Sensing, Imaging for Diagnostic and Targeted Drug Delivery for Therapeutic Applications, Drug Discovery and Development-Oresent and Future, pp. 463-488, www.intechopen.com
[19] David D. Evanoff,Jr. And George Chumanov, Chem. Phys. Chem., **6**, 1221 (2005)
[20] Chih-Hsien wang and wenlung Chen, Raman characterizing Disulfide Bonds and secondary Structure of Bovine Serum Albumin, email:wlchen@mail.ncyu.edu.tw
[21] He XM, Carter DC, Atomic structure and chemistry of human serum albumin, Nature **358**, 209 (1992).
[22] Qiang Wang, Yuching Kuo, Yuwen Wang, Gyehwa Shin, Chada Ruengruglikit, Qingrong Huang, J.Phys.Chem.B **110**, 16860 (2006).
[23] M.Venkataramanan, G.Skanth, K. Bandyopadhyay, K. Vijayamohanan, T. Pradeep, Journal of Colloidal and Interface Science, **212**, 553 (1999)
[24] J.D.Beers, A.N.Parikh, S.D.Gillmor, K.M.Beardmore, R.W.Cutts, and B.I.Swanson, Stepwise Assembly of Silver (n-alkane) thiolates: An Example of Hierarchical or Cooperative Self-Assembly, Journal of Young Investigators, 1998, @jyijournal,
[25] P.restani, C.Ballabio, A.Cattaneo, P. Isoardi, I.teraciano, A. Fiocchi, Allergy, **59**(78), 21 (2004)
[26] Qiaoli Yue, Tongfei Shen, Changna Wang, Chaohui Gao, and Jifeng Liu, International Journal of Spectroscopy, Article ID 284173, 9 pages, Volume 2012
[27] Jiang Gong LIANG, Hai Yan XIE, Xin Ping AI, Zhi Ke HE, Dai Wen Pang, Chinese Chemical Letters **15** (11), 1319 (2004)
[28] Russell A.Bell, James R. Kramer, Environmental Toxicology and Chemistry, **18**(1), 9 (1999)
[29] Angelo Longo, Gianfranco Carotenuto, Mariano Palomba and Sergio De Nicola, Polymers, **3**, 1794 (2011)
[30] K. Michaelian, N. Rendon, I.L.Garzon, Phys.Rev.B, **60(**3), 1999 (1999).
[31] Daniel G. Isom, Carlos A. Castaneda, Brian R. Cannon, Priya D. Velu, Bertrand Garcia-Moreno E., Charges in the hydrophobic interior of proteins, PNAS, **107**(37), 16096 (2010)
[32] D. Chakravorty, S. Basu, B. N. Pal, P. K. Mukherjee, B. Ghosu, K. Chatterjee, A. Bose, S. Bhattacharya, A. Banerjee, Bull.Mater.Sci. **31**(3), 263 (2008).